EurJOC
European Journal of Organic Chemistry

Full Papers
doi.org/10.1002/ejoc.202100546

Chemistry Europe
European Chemical Societies Publishing

Special Collection

Microwave-Assisted 1,3-Dipolar Cycloaddition of Azomethine Ylides to [60]Fullerene: Thermodynamic Control of Bis-Addition with Ionic Liquids Additives

Estefanía M. Martinis,[a, b] Alejandro Montellano,[c] Andrea Sartorel,[a] Mauro Carraro,*[a] Maurizio Prato,*[c, d, e] and Marcella Bonchio*[a]

Dedicated to Professor Franco Cozzi on the occasion of his 70th birthday.

The cycloaddition of azomethine ylides to [60]fullerene (C_{60}) has been studied in ortho-dichlorobenzene (*o*-DCB) by evaluating the impact of an ionic liquid (IL) additive. The solvent effect has been addressed by evaluating the activation parameters of the cycloaddition and the boosting effect of the microwave (MW) induced dielectric heating. The IL additive plays a twofold role of stabilizing the dipolar ylide intermediate and favoring the retro-cycloaddition at high temperature regime. Under the conditions explored, a combined kinetic and thermodynamic preference favors the selective formation of *trans* bis-fulleropyrrolidine regioisomers, in agreement with the DFT computational analysis.

Introduction

Fullerene functionalization by the azomethine ylide cycloaddition, yielding fulleropyrrolidines (FPs),[1] has significantly contributed to the synthesis of new molecular materials for transformative research in strategic fields, including solar energy conversion and nanomedicine.[2] FPs synthesis tolerates many functional groups and can be accelerated by microwave (MW) irradiation.[3,4] In this case, toluene, benzene or *o*-dichlorobenzene (*o*-DCB) have been used as solvents, whereby the latter displays a relatively higher boiling point and medium MW-absorbing properties (with a tangent loss, tan $\delta = 0.280$, higher than that of water, tan $\delta = 0.123$).[5] Moreover, we have previously described the preparation of FPs in a mixture of ionic liquids (ILs) and *o*-DCB, showing that higher reaction rates and conversions can be achieved in such conditions.[6,7] The use of ILs is aimed at addressing the replacement of hazardous volatile organic solvents, being instrumental for fast and selective MW-heating by ionic conduction, with negligible vapor pressure and safer protocols.[8]

In this work, we have investigated the effect of MW irradiation on the cycloaddition of azomethine ylides to [60] fullerene, in *o*-DCB/IL mixtures (Scheme 1), in order to address the thermal effect of MW-irradiation on reaction rates and selectivity. When the 1,3-dipolar cycloaddition is carried out on the fullerene sphere, indeed, not only the mono-adduct (m-FP) is obtained, but a complex mixture of poly-adducts (p-FP) can also form at higher fullerene conversion. Thus, 8, 46 and 262 FP regioisomers can be expected for symmetrical addends respectively for the bis, tris and tetrakis- addition at the fullerene core.

FP bis-adducts, in particular, are of great interest in a wide number of applications in materials science.[9] However, their

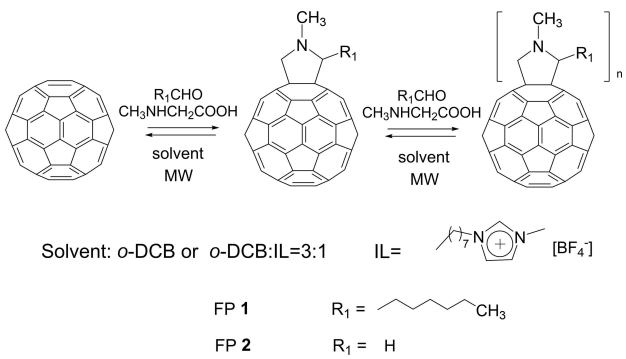

Scheme 1. Azomethine ylide cycloaddition to [60]fullerene yielding mono- and poly-adducts (FPs **1** and **2**) by reacting heptaldehyde or formaldehyde respectively, under MW irradiation, in *o*-DCB/IL mixtures.

[a] *Dr. E. M. Martinis, Prof. A. Sartorel, Prof. M. Carraro, Prof. M. Bonchio*
Department of Chemical Sciences, University of Padova, and ITM-CNR
Via Marzolo, 1, 35131 Padova, Italy
E-mail: mauro.carraro@unipd.it
marcella.bonchio@unipd.it
[b] *Dr. E. M. Martinis*
Faculty of Engineering - National University of Cuyo - National Scientific and Technical Research Council
Centro Universitario, M5502JMA, Mendoza, Argentina
[c] *Dr. A. Montellano, Prof. M. Prato*
Department of Chemical and Pharmaceutical Sciences, University of Trieste
Via Giorgieri 1 - 34127 Trieste, Italy
E-mail: prato@units.it
[d] *Prof. M. Prato*
Center for Cooperative Research in Biomaterials (CIC biomaGUNE),
Basque Research and Technology Alliance (BRTA)
Paseo de Miramón182, 20014 Donostia San Sebastián, Spain
[e] *Prof. M. Prato*
Basque Foundation for Science
Ikerbasque, Bilbao 48013, Spain

Supporting information for this article is available on the WWW under https://doi.org/10.1002/ejoc.202100546

Part of the "Franco Cozzi's 70th Birthday" Special Collection.

isolation and purification may be difficult and time-consuming. In this context, several approaches have been developed to increase the selectivity of bis-addition to the fullerene core.[10] While fullerene cyclopropanation has been successfully controlled with tether-directed covalent methods, supramolecular masks or photo-triggers,[11] to the best of our knowledge, there are no precedent reports on how to direct and optimize the bis-addition selectivity during FPs synthesis.

Our results address: (i) the impact of MW-assisted heating on the cycloaddition kinetics and selectivity in *o*-DCB and IL containing media; (ii) optimization of the synthetic protocol towards the bis-substitution of the fullerene core; (iii) DFT calculations to interrogate mechanism and the thermodynamic drivers leading to stable FP bis-adducts.

Results and Discussion

The reactivity of [60]fullerene with sarcosine and heptaldehyde was initially used as a benchmark reaction to screen the influence of the synthetic conditions. In particular, we focused on the use of MW-activated IL phases to accelerate the azomethine ylide cycloaddition and control the formation of fullerene poly-adducts, p-FP **1** (Scheme 1).

IL nature and content, as well as [60]fullerene concentration were shown to affect both the yield and the selectivity of the reaction.[7] In particular, long chain ILs are effective to improve fullerene dispersion. Therefore, a 1-methyl-3-*n*-octyl imidazolium tetrafluoroborate (OmimBF$_4$): *o*-DCB = 1:3 mixture was used to prevent clustering/aggregation phenomena, and the [60]fullerene concentration was set to ensure its complete solubilization, while yield optimization was explored as a function of the relative ratio between azomethine ylide precursors, sarcosine and heptaldehyde. A faster conversion of pristine [60]fullerene to m-FP **1** was thus observed at a fullerene concentration of 7 mM, in the presence of two and four equivalents of sarcosine and heptaldehyde, respectively.

ILs are known to play a role in the stabilization of the incipient 1,3-dipole intermediate, however favoring cyclo-reversion[6,12–14] under MW-induced dielectric heating. Indeed, the cyclo-reversion of FPs can be readily achieved in pure ILs under MW irradiation by unlocking the pyrrolidine ring to back-release pristine [60]fullerene.[6] Noteworthy, when *o*-DCB is introduced as a co-solvent, retro-cycloaddition is remarkably slowed down, which provides a facile control over the process reversibility giving access to a thermodynamic equilibration of the reaction.

The effect of the temperature on the reaction was initially investigated under conventional heating, in a temperature range between 343 and 443 K, in the absence of MW irradiation, using *o*-DCB, either alone or with the IL additive, as the solvent phase.

Table 1 collects the first order rate constants (k_{obs}) obtained for [60]fullerene conversion under the explored reaction conditions (Scheme 1).

The experimental kinetics show the progress of [60]fullerene cycloaddition, which generally occurs with consecutive formation of m-FP **1** and p-FP **1** products (Figures S1–S12).

A typical kinetic trace is reported in Figure 1a for the reaction carried out at 423 K (entry 5 in Table 1) in *o*-DCB, showing a [60]fullerene conversion up to 58% in 2 h, with formation of m-FP **1** (35%) and a mixture p-FP **1** (23%). When IL is added to the solvent phase, the cycloaddition kinetics is remarkably faster so that formation of p-FP **1** becomes prevalent above 400 K (Figures S10–S12). In Figure 1b is reported the corresponding kinetic trace for the reaction with IL additive, at the same temperature (423 K), showing the prevalent formation p-FP **1** (52%) vs. m-FP **1** (39%) in 60 min. Noteworthy, the IL additive leads to a 4-fold increase of the reaction rate with respect to the control reaction in pure *o*-DBC at 443 K (R_{obs} = 17.3 and 3.77 μmol L^{-1} s^{-1}, respectively), with [60]fullerene conversion rising up to 64% in 5 minutes (Table 1, entry 12 vs. entry 6).

The Eyring plot in Figure 2 reports the dependence of the reaction kinetic constant (k_{obs}) on the temperature conditions (Table 1), according to Equation (1):

Table 1. Reaction rate and conversion, observed during the reaction of [60]fullerene with sarcosine and heptaldehyde in *o*-DCB and *o*-DCB:IL 3/1 v/v.

Entry[a]	Solvent	T [K]	R_{obs} [μMs^{-1}] [$k_{obs}\times10^5$/s^{-1}][b]	[%] Conv.[c] 5 min	60 min
1	*o*-DCB	343	0.19 (2.7)	1	5
2	*o*-DCB	363	0.40 (5.7)	2	10
3	*o*-DCB	383	0.83 (7.7)	4	38
4	*o*-DCB	403	1.42 (20.3)	6	45
5	*o*-DCB	423	2.51 (35.8)	11	50
6	*o*-DCB	443	3.77 (53.8)	16	52
7	IL 25%	343	1.0 (14)	4	12
8	IL 25%	363	2.1 (29)	9	48
9	IL 25%	383	5.4 (78)	24	58
10	IL 25%	403	9.1 (130)	39	82
11	IL 25%	423	13.7 (196)	59	86
12	IL 25%	443	17.3 (247)	64	88

[a] In all reactions: [60]fullerene 7 mM, sarcosine 14 mM, heptaldehyde 28 mM. Entries 1–6: reaction performed in 1 mL *o*-DCB; entries 7–12: reactions performed in 0.8 mL with ratio *o*-DCB/IL 3/1 v/v; [b] R_{obs} = initial reaction rates calculated from a linear regression at conversion < 20%; k_{obs} is the first order rate constant obtained by dividing R_{obs} for the initial concentration of [60]fullerene, equal to 7 mM. [c] [60]fullerene conversion monitored by HPLC analysis.

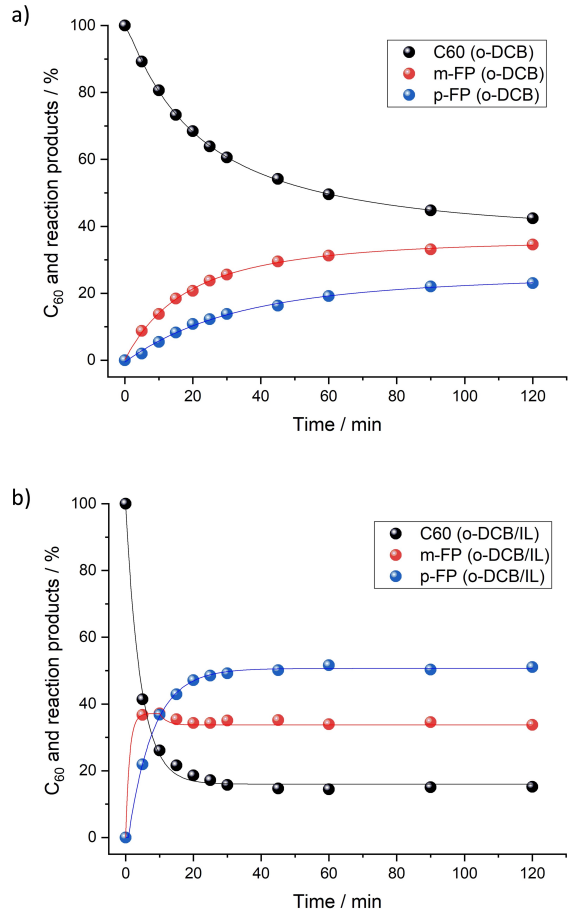

Figure 1. Kinetic traces of [60]fullerene conversion to m-FP **1** and p-FP **1** during 1,3-dipolar cycloaddition of sarcosine and heptaldehyde in 1 mL of *o*-DCB (a) or 0.8 mL of *o*-DBC/IL 3/1 v/v (b), at 423 K. [60]fullerene 7 mM; sarcosine 14 mM, heptaldehyde 28 mM. Data are connected with continuous lines for a better visualization.

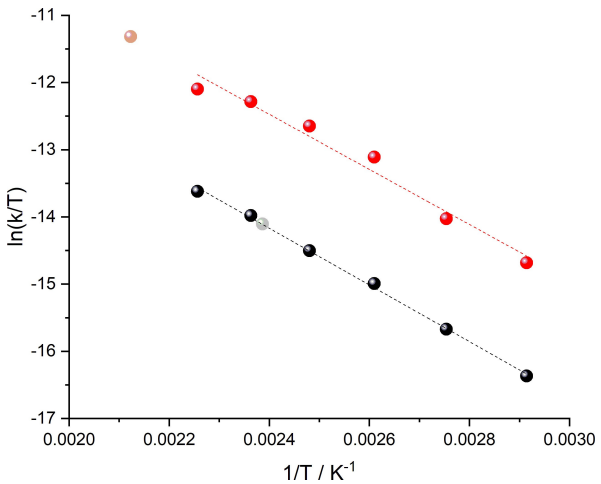

Figure 2. Eyring plot for the reaction performed under conventional heating conditions, in o-DCB (black circles) and in the presence of 25 % $OmimBF_4$ (red circles). MW-induced T_{calc} (Table 2) were extrapolated from this graph (light grey and red circles).

$$ln(k_{obs}/T) = -\frac{\Delta H^{\ddagger}}{R}\frac{1}{T} + \frac{\Delta S^{\ddagger}}{R} + \ln\left(\frac{Kk_B}{h}\right) \quad (1)$$

where $\Delta H^{\ddagger}$ and $\Delta S^{\ddagger}$ are the enthalpy and entropy of activation, respectively, T is the reaction absolute temperature, R is the gas constant (1.986 Kcalmol^{-1}), K is the transmission coefficient (assumed to be 1), k_B = Boltzmann constant, h = Planck constant.

In all cases, k_{obs} values are obtained considering first order kinetics for the [60]fullerene reactant, in agreement with the experimental concentration-time profiles and consistent with the generally accepted mechanistic scheme (Table 1 and Scheme S1 in Supporting Information).

Inspection of graphs in Figure 2 shows the line slopes (ca. 4200 K^{-1}) yielding similar values of activation enthalpy, $\Delta H^{\ddagger}$ = 8.4 ± 0.2 and 8.0 ± 0.8 Kcalmol^{-1} ascribed to *o*-DCB and *o*-DCB/IL solvent conditions, respectively. Similarly, the activation entropies are calculated from the graph intercepts, showing large negative values, that turn out to be slightly mitigated by the addition of the IL additive ($\Delta S^{\ddagger}$ = −55.2 ± 0.5 and −52.3 ± 1.7 calK^{-1}mol^{-1} for *o*-DCB and *o*-DCB/IL, respectively). The almost identical enthalpy activation barriers together with the negative activation entropy are consistent with a concerted 1,3-dipolar cycloaddition mechanism. The rate enhancement, observed in the presence of ILs, is therefore explained by a less negative activation entropy in the presence of ILs, due a favorable desolvation of the cyclic transition state with respect to the zwitterionic azomethine ylide reagent (Scheme S1).[15]

With the aim to exploit the ILs ionic phase as excellent MW-absorbers, the reaction was performed under MW irradiation (50 W), flowing compressed air to avoid possible overheating effects (Table 2).

MW-assisted kinetics were instrumental to address the temperature conditions operating under MW induced dielectric heating. The operating temperature can be determined indirectly by extrapolation of the Eyring plot in Figure 2 (T_{calc} in Table 2).[16,17]

The combined use of IL and MW is responsible for a remarkable initial rate acceleration, reaching up to 40.1 μM s^{-1} (Figure S13). This kinetic effect (k_{obs} = 573 × 10^{-5} s^{-1}) corresponds to a temperature read-out T_{calc} = 471 K, as provided by the

Table 2. Rate, [60]fullerene conversion to m-FP **1**, and selectivity ratio, observed for the MW-assisted reaction of [60]fullerene with sarcosine and heptaldehyde in *o*-DCB and *o*-DCB:IL = 3:1.

#[a]	Solvent	Conv. (%) C_{60}[b]	m-FP **1** (%)[c]	Sel[d]	R_{obs} (μM s^{-1}) (k_{obs} × 10^5/s^{-1})	T_{calc} (K)[e]
1	*o*-DCB	9	6.6	4	2.2 (31)	419
2	IL 25 %	65	31.7	1	40.1 (573)	471

[a] In all reactions: [60]fullerene 7 mM; sarcosine 14 mM, heptaldehyde 28 mM. 50 W power applied under magnetic stirring and simultaneous cooling by compressed air at 40 psi. Entry 1: reaction performed in 1 mL *o*-DCB; entry 2: reaction performed in 0.8 mL *o*-DCB/IL 3/1 v/v. [b] [60]fullerene conversion monitored by HPLC analysis after 5 min. [c] % of m-FP **1** monitored by HPLC analysis after 5 min. [d] Selectivity ratio, calculated as m-FP **1**/p-FP **1** ratio. [e] Temperature extrapolated from the Eyring plot in Figure 2.

Eyring linear relationship in Figure 2 (light red circle). With respect to the control reaction, performed in pure *o*-DCB and under analogous MW irradiation power, the IL additive leads to a ca. 20-fold rate acceleration, which is explained considering a poor dielectric heating of the pure *o*-DCB solvent (T_{calc} = 419 K, light grey circle in Figure 2). Despite the MW-induced boosting effect, [60]fullerene conversion levels off at 65% (Figure S13 and Table 2) with formation of both m-FP **1** and p-FP **1** in ca. 1.1 ratio (Table 2). While the evolution to poly-substituted products is expected to increase at higher [60]fullerene conversion (Figure 1 and Table 2), the observation of a limiting plateau yield is likely ascribed to the equilibrium regime involving the thermally activated retro-cycloaddition. This latter is effective in the presence of the IL additive and likely occurs at all the fulleropyrrolidine sites.

To further explore the effect of the thermodynamic control on the cycloaddition products, we turned our attention to the regioselectivity of the 1,3-dipolar cycloaddition obtained with sarcosine and formaldehyde as a model reaction, yielding FPs **2** (Scheme 1).[18] In particular, the N-methyl unsubstituted azomethine ylide generated from formaldehyde rules out the formation of additional bis-FP **2** stereoisomers and minimizes the steric hindrance of a second pyrrolidine ring installed on the C_{60} scaffold.[19]

1,3 dipolar cycloaddition on [60]fullerene can involve 30 reactive double bonds, shared by condensed [6,6] cycles, so that after installation of the first pyrrolidine ring, 8 isomeric bis-adducts can be formed, either located on the same C_{60} hemisphere with respect to the first functionalization (three *cis* isomers), in the opposite one (four *trans* isomers), or at the equatorial positions (1 *eq* isomer) (Figure 3).[19]

With the aim to tune the selectivity of the bis-cycloaddition, MW-irradiation was optimized at an applied power of 12 W, and the product profile was monitored via HPLC analysis, by identification of the single analytes specifically attributed to m-FP **2** and to *trans*-, *cis*- and *equatorial* bis-fulleropyrrolidines (Figures S14 and attributions in Table S1), while considering the remaining peaks as an overall signature of further [60]fullerene poly-functionalization. Using pure *o*-DCB as solvent, a complex mixture of fulleropyrrolidines readily forms in solution after ca. 10 min irradiation (Figure S14a). Analysis of the product profile reveals that [60]fullerene conversion (>80%) leads to the formation of m-FP **2** (13%) together with seven bis-FP **2** regioisomers (31%) where *trans*-bis-fulleropyrrlidines are the prevalent isomers (23%). In this reaction, a mixture of ill-defined p-FP **2** turns out to be dominant (56%), hampering the isolation of desired bis-functionalized products (Figure 4, trace a). A similar product distribution is also obtained under conventional heating conditions.

Noteworthy, the introduction of the ionic liquid additive combined with MW-induced dielectric heating was crucial for the simplification of the product profile. At shorter irradiation time (<5 min), [60]fullerene conversion remains below 60%, which limits the formation of p-FP **2**, while enhancing the production of m-FP **2** (46%) and of bis-FP **2** where the preferential selectivity towards *trans* and *equatorial* regioisomers is confirmed (54%) (Figure S14b and Figure 4, trace b). The selective formation of *trans* and *equatorial* regioisomers at short reaction time, is indicative of a marked kinetic preference, regulated by steric hindrance that favors the bis-functionalization at the equatorial or sub-hemisphere distal positions.[19]

To verify a converging thermodynamic control over the equilibration of bis-fulleropyrrolidine regioisomers, we designed a two-stage/follow-up experiment. In the first stage, a crude reaction mixture was obtained under MW irradiation (12 W, <10 min) in pure *o*-DCB and purified from the unreacted ylide precursors. The "purified" crude was then irradiated again, in a second stage (12 W for 5 minutes), using a *o*-DCB:IL = 3:1 solvent phase. HPLC analysis confirmed that the initial mixture (Figure 5a), containing the unreacted [60]fullerene and fulleropyrrolidine products (m-FP **2**, and seven bis-FP **2** regioisomers),[20] evolved in the second stage, under thermodynamic re-equilibration. The resulting product profile shows an increased conversion of [60]fullerene (up to 95%) that occurs by consuming the *trans*-4, *cis* 1–3 and *eq* isomers while leading

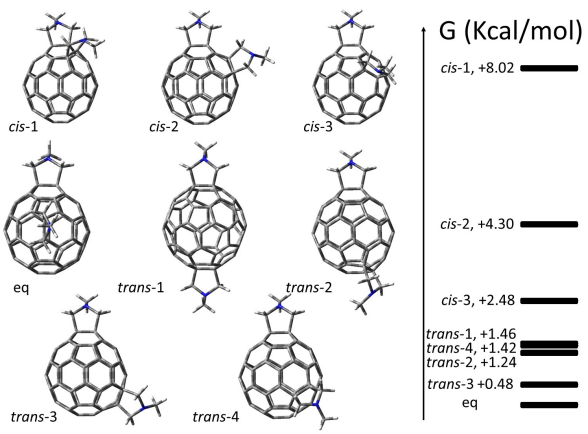

Figure 3. Isomeric bis-fulleropyrrolidines (bis-FP **2**) and their relative Gibbs free energy (see main text).

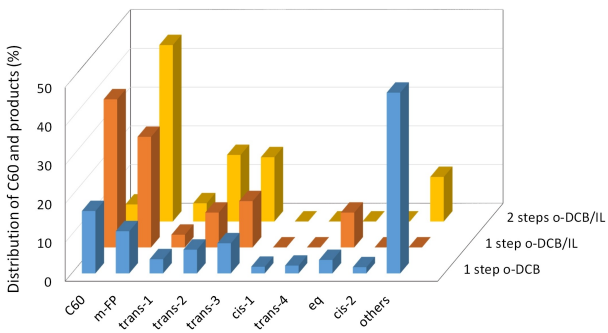

Figure 4. Histogram plot illustrating the % composition of the reaction mixtures obtained with 14 μmol of [60]fullerene, 56 μmol of formaldehyde and 28 μmol of sarcosine, irradiated at 12 W in (a) 2 mL of o-DCB, >10 min (1 step *o*-DCB, blue columns) or (b) in 1.5 mL of o-DCB and 0.5 mL of $OmimBF_4$, 5 min (1 step *o*-DCB/IL, orange columns). Yellow columns (c) are referred to an ylide precursors-free mixture, obtained from the reaction in *o*-DCB, after thermodynamic equilibration in 1.5 mL of *o*-DCB and 0.5 mL of $OmimBF_4$, upon 5 min irradiation (2 steps *o*-DCB/IL). In all cases, % are based on chromatographic peak areas by assuming a similar response factor for all compounds.

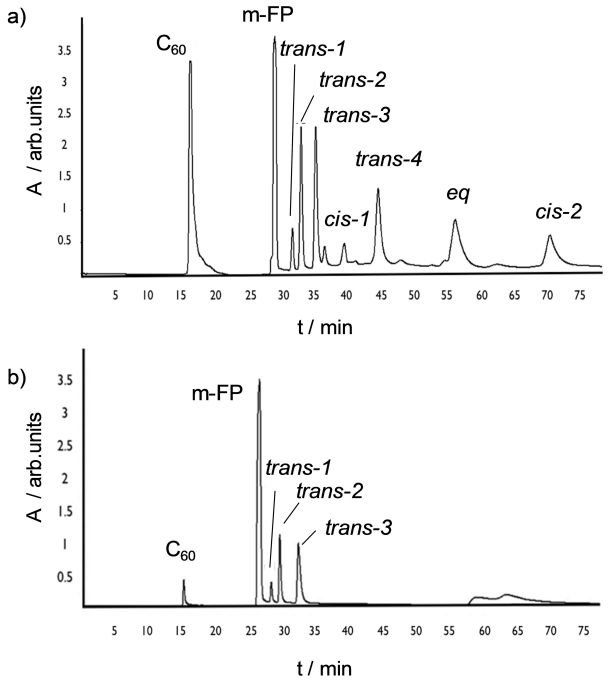

Figure 5. HPLC profile of (a) a mixture of [60] fullerene monoadduct (m-FP **1**) and bis-adducts obtained from a reaction of 14 μmol of fullerene, 56 μmol of formaldehyde and 28 μmol of sarcosine irradiated at 12 W in 2 mL of *o*-DCB (< 10 min) and (b) of the mixture in (a) after irradiation (12 W for 5 min) in 1.5 mL of *o*-DCB and 0.5 mL of $OmimBF_4$.

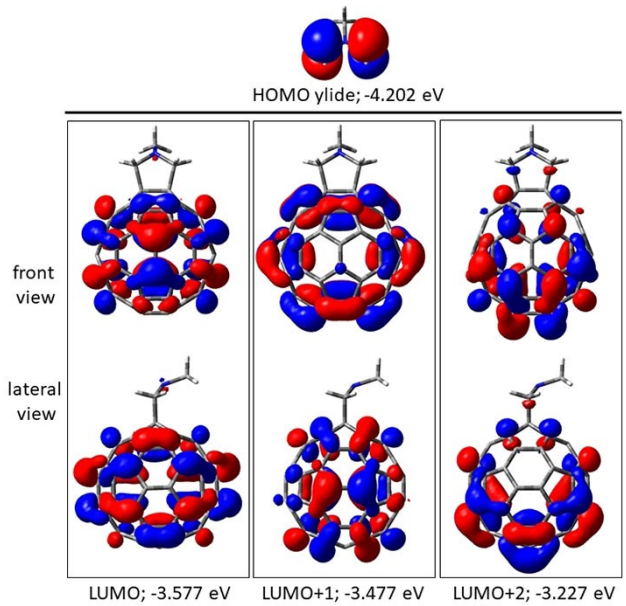

Figure 6. Representation of frontier molecular orbitals of m-FP **2** (LUMO, LUMO + 1 and LUMO + 2) and of ylide (HOMO).

Table 3. Frontier empty orbitals of m-FP **2**, their difference in energy with respect to the HOMO of the ylide reagent, and preferred bis-FP **2** regioisomers localized on the [60]fullerene scaffold (minor regioisomers are indicated in brackets deriving from a less favourable interaction of the orbital density), see Figure 6.

Frontier Orbital of m-FP **2**	Gap in energy with HOMO of ylide [eV] ([Kcal/mol] in brackets)	Preferred bis-FP **2** regioisomers based on a HOMO-ylide controlled orientation
LUMO	0.625 (14.4)	*cis*-2, *eq*, *trans*-3 (*cis*-3)
LUMO + 1	0.724 (16.7)	*cis*-1, *eq*, *trans*-2
LUMO + 2	0.975 (22.5)	*trans*-1, *trans*-4 (*cis*-3, *trans*-2, *trans*-3)

to the preferential formation of *trans*-1, *trans*-2, *trans*-3 bis-FP **2** regioisomers (Figure 4, trace c and Figure 5b). The further progress of the 1,3 dipolar cycloaddition, without recharging the ylide precursors (Scheme 1), is indicative of a reversible reaction pathway under thermodynamic control.

To address reaction path and product distribution, we performed DFT calculation at the b3lyp/6-311G level (see Figure 3, Figure 6, Figure S15, Figure S16).

The formation of bis-fulleropyrrolidines results from the favorable interaction between empty orbitals of the m-FP **2** (in particular, the LUMO, LUMO + 1 and LUMO + 2) and the HOMO of the ylide reagent, with a calculated energy gap in the range 0.625–0.975 eV (14.4–22.5 Kcal mol^{-1}, Figure 6 and Table 3).

Geometry optimization of all the expected bis-FP **2** has been performed with the aim to address their relative thermodynamic stability. In all cases the calculated free energies (ΔG) of the diverse regioisomers are referred to the most stable equatorial bis-FP **2** (*eq*, Figure 3).

Indeed, the LUMO-LUMO + 2 molecular orbitals of m-FP **2** display an electron density distribution involving diverse [6,6] bonds of the fullerropyrrolidine scaffold, which provides a rational for a regioselective 1,3-dipolar cycloaddition controlled by the frontier orbital coefficients of the interacting species (Figure 6 and Table 3).[21]

According to the computational analysis, the higher energy bis-FP **2** isomers display a cis-orientation (*cis*-1, *cis*-2 and *cis*-3) with relative energy gap in the range ΔG = + 2.5–8.0 Kcal mol^{-1}.

Because of the lower distortion of the fullerene scaffold, bis-FP **2** with a *trans*-orientation are more stable regioisomers, with similar energy content (ΔG below 1.5 Kcal mol^{-1}, thus at the limit of the significance value for this level of calculation).

These results are in good agreement with the regioselectivity outcome observed under diverse heating conditions, indicating that the *trans*- bis-FP **2** isomers are the dominant products, formed under thermodynamic control, by unlocking the cyclo-reversion of the high energy *cis*-isomers (Figure 4 and Figure 5).

Conclusion

The functionalization of [60]fullerene by azomethine ylide 1,3-dipolar cycloaddition to fulleropyrrolidines has been performed by the combined use of IL phases and MW dielectric heating. The reaction of [60]fullerene with heptaldehyde and sarcosine as ylide precursors has been considered as a benchmark system

to address the cycloaddition performance under conventional heating and under MW irradiation. Here, the use of the IL additive allows a flash thermal activation induced by the efficient MW absorption, which is responsible for a 20-fold rate acceleration of [60]fullerene conversion. Inspection of the activation parameters by the Eyring relationship points to a favourable stabilization of the zwitterionic azomethine ylide reagent in the presence of ILs, which mitigates the negative activation entropy expected for the evolution of the cyclic transition state. Optimized conditions were then applied for the regioselective formation of bis-FP **2** *trans*-regioisomers, as observed for the reaction of [60]fullerene with a symmetrical ylide generated in situ from formaldehyde and sarcosine precursors. In this case, the combined use of ILs additive and MW irradiation is effective to unlock the reverse regime of retro-cycloaddition, thus allowing a desirable thermodynamic control of the product distribution. Controlling [60]fullerene functionalization by a proper choice of the solvent composition and of the temperature conditions offers a straightforward tool to exploit a convergent kinetic and thermodynamic control on the cycloaddition selectivity.

Experimental Section

General: Continuous microwave irradiation was carried out in a CEM-Discover-Coolmate mono-modal microwave apparatus, with simultaneous monitoring of irradiation power, pressure and temperature. Compressed air was applied to improve the temperature control of the reaction mixtures. All reactions were monitored by HPLC, using a Shimadzu LC-10AT VP pump system, equipped with a UV detector SPD-10A VP set at 340 nm. Phenomenex Luna and Cosmosil Buckyprep columns (250×4.6 mm 5 μm particles) were used, with toluene as eluent flowing at 1 mL/min.

Procedure for the cycloadditions: Unless otherwise stated, 5 mg of [60]fullerene (7 μmol) were dispersed upon sonication in a mixture of *o*-dichlorobenzene (and ionic liquid), together with sarcosine (1.2 mg, 14 μmol) and aldehyde (3.2 mg, 28 μmol), in a closed glass test tube containing 1 mL of solvent. Samples were diluted using toluene and analyzed by HPLC.

DFT calculations have been performed with Gaussian 09 software. Geometries have been optimized at the b3lyp/6-311G level in the gas phase. Inclusion of a continuous pcm model for the solvent (water) did not lead to significant changes in the relative energies of the bis-adducts discussed in Figure 3.

Acknowledgements

We thank Martino Gardan for preliminary investigation. Funding from MIUR (PRIN Nanoredox, Prot. 2017PBXPN4) is gratefully acknowledged. A.S. acknowledges Fondazione Cariparo for funding (project SYNERGY, Ricerca Scientifica di Eccellenza 2018). This work was performed under the Maria de Maeztu Units of Excellence Program from the Spanish State Research Agency – Grant No. MDM-2017-0720.

Conflict of Interest

The authors declare no conflict of interest.

Keywords: 1,3-Dipolar cycloaddition · Fullerenes · Ionic liquids · Microwaves · Temperature effect

[1] a) M. Maggini, G. Scorrano, M. Prato, *J. Am. Chem. Soc.* **1993**, *115*, 9798–9799; b) M. Prato, M. Maggini, *Acc. Chem. Res.* **1998**, *31*, 519–526; c) N. Tagmatarchis, M. Prato, *Synlett* **2003**, *6*, 768–779.
[2] a) M. Prato, *J. Mater. Chem.* **1997**, *7*, 1097–1109; b) A. Montellano López, A. Mateo-Alonso, M. Prato, *J. Mater. Chem.* **2011**, *21*, 1305–1318; c) M. Prato, *Top. Curr. Chem.* **1999**, *199*, 173–187; d) A. Mateo-Alonso, C. Sooambar, M. Prato, *Org. Biomol. Chem.* **2006**, *4*, 1629–1637; e) A. Mateo-Alonso, D. M. Guldi, F. Paolucci, M. Prato, *Angew. Chem. Int. Ed.* **2007**, *46*, 8120–8126; *Angew. Chem.* **2007**, *119*, 8266–8272; f) A. V. Mumyatov, A. E. Goryachev, F. A. Prudnov, O. A. Mukhacheva, D. K. Sagdullina, A. V. Chernyak, S. I. Troyanov, P. A. Troshin, *Synth. Met.* **2020**, *270*, 116565; g) R. Tao, T. Umeyama, K. Kurotobi, H. Imahori, *ACS Appl. Mater. Interfaces* **2014**, *6*, 17313–17322; h) M. A. Faist, S. Shoaee, S. Tuladhar, G. F. A. Dibb, S. Foster, W. Gong, T. Kirchartz, D. D. C. Bradley, J. R. Durrant, J. Nelson, *Adv. Energy Convers.* Mater. **2013**, *6*, 744–752; i) W. Huang, E. Gann, N. Chandrasekaran, S. K. K. Prasad, S.-Y. Chang, L. Thomsen, D. Kabra, J. M. Hodgkiss, Y.-B. Cheng, Y. Yang, C. R. McNeill, *Adv. Energy Mater.* **2017**, *7*, 1602197; j) N. C. Miller, S. Sweetnam, E. T. Hoke, R. Gysel, C. E. Miller, J. A. Bartelt, X. Xie, M. F. Toney, M. D. McGehee, *Nano Lett.* **2012**, *12*, 1566–1570; k) J. K. Sørensen, J. Fock, A. H. Pedersen, A. B. Petersen, K. Jennum, K. Bechgaard, K. Kilså, V. Geskin, J. Cornil, T. Bjørnholm, M. B. Nielsen, *J. Org. Chem.* **2011**, *76*, 245–263.
[3] a) F. Langa, P. de la Cruz, *Comb. Chem. High Throughput Screening* **2007**, *10*, 766–782; b) F. Langa, P. de la Cruz, in: *Microwaves in Organic Synthesis* (Ed. A. Loupy), Wiley-VCH, and references therein.
[4] a) P. de la Cruz, A. de la Hoz, F. Langa, B. Illescas, N. Martin, *Tetrahedron* **1997**, *53*, 2599–2608; b) S. Wang, J.-m. Zhang, L.-p. Song, H. Jiang, S.-Z. Zhu, *J. Fluorine Chem.* **2005**, *126*, 349–353; c) J. Safaei-Ghomi, R. Masoomi, *RSC Adv.* **2015**, *20*, 15591–15596; d) B. Jin, R.-F. Peng, W.-N. Yang, K. Wang, B.-Q. Yuan, S.-J. Chu, *Synth. Commun.* **2010**, *40*, 580–586; e) J. Zhang, W. Yang, P. He, S. Zhu, S. Wang, *Synth. Commun.* **2005**, *35*, 89–96; f) F. G. Brunetti, M. A. Herrero, J. de M Muñoz, A. Díaz-Ortiz, J. Alfonsi, M. Meneghetti, M. Prato, E. Vázquez, *J. Am. Chem. Soc.* **2008**, *130*, 8094–8100; g) E. Vazquez, F. Giacalone, M. Prato, *Chem. Soc. Rev.* **2014**, *43*, 58–69.
[5] V. G. Gude, *Microwave-Mediated Biofuel Production*, CRC Press, Boca Raton, **2017**, p. 38.
[6] I. Guryanov, A. Montellano Lopez, M. Carraro, T. Da Ros, G. Scorrano, M. Maggini, M. Prato, M. Bonchio, *Chem. Commun.* **2009**, 3940–3942.
[7] I. Guryanov, F. M. Toma, A. Montellano Lopez, M. Carraro, T. Da Ros, G. Angelini, E. D'Aurizio, A. Fontana, M. Maggini, M. Prato, M. Bonchio, *Chem. Eur. J.* **2009**, 12837–12845.
[8] a) Z. Yinghuai, S. Bahnmueller, C. Chibun, K. Carpenter, N. S. Hosmane, J. A. Maguire, *Tetrahedron Lett.* **2003**, *44*, 5473–5476; b) Z. Yinghuai, *J. Phys. Chem. Solids* **2004**, *65*, 349–353; c) R. R. Deshmukh, J. W. Lee, U. S. Shin, J. Y. Lee, C. E. Song, *Angew. Chem. Int. Ed.* **2008**, *47*, 8615–8617; *Angew. Chem.* **2008**, *120*, 8743–8745.
[9] a) F. Zhang, W. Shi, J. Luo, N. Pellet, C. Yi, X. Li, X. Zhao, T. J. S. Dennis, X. Li, S. Wang, Y. Xiao, S. M. Zakeeruddin, D. Bi, M. Grätzel, *Adv. Mater.* **2017**, *29*, 1606806; b) T. Umeyama, H. Imahori, *Acc. Chem. Res.* **2019**, *52*, 2046–2055.
[10] D. Sigwalt, F. Schillinger, S. Guerra, M. Holler, M. Berville, J.-F. Nierengarten, *Tetrahedron Lett.* **2013**, *54*, 4241–4244.
[11] L. Đorđević, L. Casimiro, N. Demitri, M. Baroncini, S. Silvi, F. Arcudi, A. Credi, M. Prato, *Angew. Chem. Int. Ed.* **2021**, *60*, 313–320; *Angew. Chem.* **2021**, *133*, 317–324.
[12] A. Alvarez, E. Ochoa, Y. Verdecia, M. Suárez, M. Sola, N. Martín, *J. Org. Chem.* **2005**, *70*, 3256–3262.
[13] O. Lukoyanova, C. M. Cardona, M. Altable, S. Filippone, A. Martín-Domenech, N. Martín, L. Echegoyen, *Angew. Chem. Int. Ed.* **2006**, *45*, 7430–7433; *Angew. Chem.* **2006**, *118*, 7590–7593.
[14] a) S. Filippone, M. Izquierdo Barroso, Á. Martín-Domenech, S. Osuna, M. Solà, N. Martin, *Chem. Eur. J.* **2008**, *14*, 5198–5206; b) N. Martín, M.

Altable, S. Filippone, A. Martín-Domenech, L. Echegoyen, C. M. Cardona, *Angew. Chem. Int. Ed.* **2006**, *45*, 110–114; *Angew. Chem.* **2006**, *118*, 116–120.
[15] T. Rispens, J. B. F. N. Engberts, *J. Phys. Org. Chem.* **2005**; *18*, 908–917.
[16] P. K. Chen, M. R. Rosana, G. B. Dudley, A. E. Stiegman, *J. Org. Chem.* **2014**, *79*, 7425–7436.
[17] M. A. Frasso, A. E. Stiegman, G. B. Dudley, *Chem. Commun.* **2020**, *56*, 11247–11250.
[18] a) K. Kordatos, S. Bosi, T. Da Ros, A. Zambon, V. Lucchini, M. Prato, *J. Org. Chem.* **2001**, *66*, 2802–2808; b) S. Marchesan, T. Da Ros, M. Prato, *J. Org. Chem.* **2005**, *70*, 4706–4713.
[19] Y. Nakamura, K. O-kawa, J. Nishimura, *Bull. Chem. Soc. Jpn.* **2003**, *76*, 865–882.
[20] Under thermal conditions, 1,3 dipolar cycloaddition to [60]fullerene yields a product distributions that is similar to what observed under MW irradiation in the absence of the IL additive (compare Figure 5a with Figure 2 in ref [18b]).
[21] M. Kissane, A. R. Maguire, *Chem. Soc. Rev.* **2010**, *39*, 845–883.

Manuscript received: May 1, 2021
Revised manuscript received: May 28, 2021
Accepted manuscript online: June 1, 2021